applied sciences

MDPI

Article

Distributed Attitude Synchronization for Spacecraft Formation Flying via Event-Triggered Control

Xiong Xie, Tao Sheng * and Liang He

College of Aerospace Science and Engineering, National University of Defense Technology, Changsha 410073, China; xiexiong1997@163.com (X.X.); heliang09@nudt.edu.cn (L.H.)
* Correspondence: shengtao-2002@163.com

Abstract: The distributed attitude synchronization control problem for spacecraft formation flying subject to limited energy and computational resources is addressed based on event-triggered mechanism. Firstly, a distributed event-driven controller is designed to achieve attitude coordination with the limitation of energy and computing resources. Under the proposed control strategy, the controller is only updated at the event triggering instants, which effectively reduces the update frequency. Subsequently, an event-triggered strategy is developed to further decrease energy consumption and the amount of computation. The proposed event-triggered function only requires the latest state information about its neighbors, implying that the trigger threshold does not need to be calculated continuously. It is shown that the triggering interval between two successive events is strictly positive, showing that the control system has no Zeno phenomenon. Moreover, the update frequency of the proposed controller can be reduced by more than 90% compared to the update frequency of the corresponding time-driven controller with an update frequency of 10 Hz by choosing appropriate control parameters and the control system can still achieve high-precision convergence. Finally, the effectiveness of the constructed control scheme is verified by numerical simulations.

Keywords: spacecraft formation flying; event-triggered strategy; attitude control; distributed control

check for updates

Citation: Xie, X.; Sheng, T.; He, L. Distributed Attitude Synchronization for Spacecraft Formation Flying via Event-Triggered Control. *Appl. Sci.* **2021**, *11*, 6299. https://doi.org/10.3390/app11146299

Academic Editor: Eyad H. Abed

Received: 18 May 2021
Accepted: 6 July 2021
Published: 7 July 2021

Publisher's Note: MDPI stays neutral with regard to jurisdictional claims in published maps and institutional affiliations.

Copyright: © 2021 by the authors. Licensee MDPI, Basel, Switzerland. This article is an open access article distributed under the terms and conditions of the Creative Commons Attribution (CC BY) license (https://creativecommons.org/licenses/by/4.0/).

1. Introduction

In the last few years, spacecraft formation flying (SFF) has become increasingly popular, owing to its wide range of applications, such as earth monitoring [1], space-based synthetic aperture radar [2], and gravitational field measurement [3]. In addition, compared with the traditional large spacecraft, SFF can bring lots of benefits, including the lower cost involved in research and development (R&D) and launching [4], better flexibility, and higher robustness [5]. In addition, the formation control of multi-spacecraft systems has been extensively studied and many outstanding contributions for SFF have been made by researchers and scholars. For example, Zhao et al. [6] designed a distributed attitude control law for SFF in the context of unknown external disturbances to ensure that attitude errors cooperatively arrive at the reference neighborhood in finite time. Zou et al. [7] constructed a novel distributed attitude consensus control algorithm with finite-time convergence for SFF via homogeneous theory under undirected communication graphs. Lin et al. [8] investigated the optimal coordinated control method of SFF subject to collision avoidance among spacecraft and proposed optimal control algorithms on the basis of the state-dependent Riccati equation to avoid collisions and achieve optimal performance states. Moreover, many advanced control schemes for single spacecraft have been given by researchers [9], but there are still many challenges in applying them to multi-spacecraft systems. Therefore, the formation control of SFF is worthy of further study.

The consensus control has received considerable attention from various scientific communities in recent years [10]. For the consensus control problem, a variety of solutions can be found in the literature. Dimarogonas et al. [11] designed a feedback control law

for multiple spacecraft systems in the case that only a certain subgroup of spacecraft have access to the main control objective. For multi-agent systems in the presence of actuator failures and unknown perturbations, Siavash et al. [12] addressed the fault-tolerant formation control problem under time-varying weighted topologies. Wang et al. [13] designed a distributed attitude cooperative control strategy for SFF systems subject to time delays and the state errors could converge to zero asymptotically under the proposed controller. Zhang et al. [14] constructed two distributed attitude synchronization control algorithms for multi-spacecraft systems subject to external disturbances to achieve attitude coordination in finite time. He et al. [15] proposed a finite-time coordinated control method for second-order multi-agent systems with disturbances to achieve the main control objectives, including collision avoidance, the compensation of uncertainties, and finite-time convergence. Lin et al. [16] developed an adaptive image-based controller for robot formation systems in the context of visibility constraints to realize the system stability.

It should be emphasized that the coordination controllers proposed in the literature [10–16] are needed to be continuously updated, which will consume lots of energy and computational resources. Although the electronic technology has developed rapidly in recent years, the computing resources on the spacecraft are still limited. Moreover, it is well known that energy on the spacecraft is very precious. In light of this, the constraints on energy and computation resources should be emphasized in the design of the consensus controller. The traditional method to decrease computing and energy resources is to make the digital controller take actions periodically. However, compared with event-triggered technology, this method has the disadvantages of lack of flexibility and scalability [17]. Therefore, the event-based control strategy has attracted extensive interest of experts and scholars, and numerous event-based research results are given by researchers. Event-triggered functions can be divided into state trigger functions [18,19], time trigger functions [20], and dynamic trigger functions [21] according to the variables on which the trigger function depends. Time trigger functions have the disadvantages of low precision in realizing state coordination and the need for global state information of the formation system, and dynamic trigger functions have the shortcoming that it is difficult to rule out Zeno behavior, while state trigger functions are convenient for the design of the control system and physical implementation. Thus, state trigger functions have been extensively utilized in the field of consensus control for SFF. Dimarogonas et al. [18] proposed two event-based control algorithms which were updated at the trigger instants of itself and its neighbors. Wang et al. [19] discussed the distributed synchronization control for nonlinear multi-agent systems subject to unknown control directions and disturbances and proposed a Zeno-free event-triggered strategy to save communication resources. However, the above event-driven strategies proposed in the literature [18,19] need to be continuously calculated in the calculation of the trigger threshold, while the continuous calculation of the event-triggered threshold consumes some resources. Scholars have given some solutions to this problem. Nowzari and Cortés [22] designed an event-based controller for first-order multi-agent systems to achieve average synchronization, and the proposed event-triggered strategy did not require consecutive status information of its adjacent agents. For linear multi-agent systems under connected undirected topologies, Wu et al. [23] constructed a feedback control strategy using the estimation of its neighbors' state information to realize state coordination. In addition, it should be noted that the controllers developed in the literature [22,23] are designed for linear systems and based on feedback control technology, which means that these controllers are not suitable for SFF systems with nonlinear characteristics. Zhang et al. [24] proposed a fault-tolerant synchronization controller for nonlinear multi-agent systems via event-triggered control, backstepping control, and adaptive control. Yi et al. [25] designed an attitude coordinated control algorithm for SFF systems in the context of limited communication resources based on sliding mode control and event-driven control. Nevertheless, there are still few research studies related to the distributed event-triggered attitude consensus control for SFF systems. Therefore, it is

highly desirable to design a novel event-based controller for nonlinear SFF systems to save resources of spacecraft in the formation.

In this paper, a novel distributed attitude coordination control scheme is constructed for SFF on the basis of the event-driven control method, such that state errors of SFF can reach the reference neighborhood around the origin cooperatively under the limitation of energy and computation resources. Firstly, a distributed event-based attitude cooperative controller is designed for SFF systems with limited energy and computation resources to achieve attitude synchronization. Subsequently, a novel event-triggering mechanism without requiring successive status of its adjacent spacecraft is established to further save energy and computing resources. Unlike the cooperative controllers developed in the literature [10–16], the event-driven coordinated controller does not need to be updated continuously, which greatly reduces energy and computational resources. In contrast to the event-based consensus controllers [18,19], the event-triggering function only relies on the latest neighbors' state information, implying that no continuous calculation is required in the calculation of the trigger condition. Compared with the event-driven coordination controllers [22,23], the event-based coordinated controller is suitable for nonlinear SFF systems.

The rest of this paper is organized as follows. Preliminary knowledge and the problem statement are presented in Section 2. Sections 3 and 4 present the event-based attitude consensus control strategy and numerical simulations, respectively. Finally, some conclusions are shown in Section 5.

2. Preliminaries and Problem Statement

2.1. Preliminaries

The following symbols are defined to express conveniently. I_n stands for the $n \times n$ identity matrix. 1_n represents a n-dimensional vector of all ones. For a vector or matrix, let $\|\cdot\|$ and $\|\cdot\|_\infty$ be its Euclidean norm and Infinity norm, respectively. For the given vector $x = [x_1, x_2, \cdots, x_n]^T \in \mathbb{R}^n$, $\dot{x}$ and $\ddot{x}$ represent its first derivative and second derivative, respectively. For an arbitrary three-dimensional vector $x = [x_1, x_2, x_3]^T \in \mathbb{R}^3$, the skew-symmetric matrix $x^\times \in \mathbb{R}^{3\times 3}$ is defined as:

$$x^\times = \begin{bmatrix} 0 & -x_3 & x_2 \\ x_3 & 0 & -x_1 \\ -x_2 & x_1 & 0 \end{bmatrix}$$

In this paper, a directed graph $G = \{V, E, A\}$ is utilized to describe the information exchange of SFF systems composed of n spacecraft. The digraph G includes a set of nodes $V = \{v_1, v_2, \cdots, v_n\}$, an edge set $E \subseteq V \times V$, and an adjacency matrix $A = [a_{ij}] \in \mathbb{R}^{n\times n}$. Edge $(v_i, v_j) \in E$ implies that node v_j can receive state information from node v_i, but not necessarily vice versa. The weighted adjacency matrix A satisfies $a_{ij} > 0$ if $(v_j, v_i) \in E$, otherwise $a_{ij} = 0$. In addition, it is assumed that self-loops are not allowed, that is, $a_{ii} = 0$. For a directed graph, a directed path from v_i to v_j is composed of a sequence of ordered edges of the form $(v_i, v_k), (v_k, v_l), \cdots, (v_m, v_j)$ and if there is a node with a directed path to any other node, the digraph is said to have a directed spanning tree. The Laplacian matrix associated with the digraph G is represented by $L = D - A \in \mathbb{R}^{n\times n}$, in which $D = diag[d_1, d_2, \cdots, d_n]$ and $d_i = \sum_{j=1}^n a_{ij}$. The Laplacian matrix L satisfies $l_{ij} = -a_{ij} \leq 0 (i \neq j)$ and $\sum_{j=1}^n l_{ij} = 0 (i = 1, \cdots, n)$, showing that zero is an eigenvalue of L with an associated eigenvector 1_p.

Assumption 1. *The digraph G has at least one directed spanning tree.*

2.2. Problem Formulation

For simpleness, formation spacecraft can be regarded as rigid bodies. For ith spacecraft, the attitude dynamics described by Modified Rodrigues Parameters (MRPs) can be described by [26]:

$$\dot{\sigma}_i = G(\sigma_i)\omega_i \tag{1}$$

$$G(\sigma_i) = \frac{1}{2}\left[\frac{1-\|\sigma_i\|^2}{2} I_3 + \sigma_i^{\times} + \sigma_i \sigma_i^T\right] \tag{2}$$

$$J_i\dot{\omega}_i = -{\omega_i}^{\times} J_i\omega_i + u_i \tag{3}$$

where $J_i \in \mathbb{R}^{3\times 3}$ refers to the inertia matrix, $u_i \in \mathbb{R}^3$ represents the control input, $\sigma_i = [\sigma_{i1}, \sigma_{i2}, \sigma_{i3}]^T \in \mathbb{R}^3$ and $\omega_i = [\omega_{i1}, \omega_{i2}, \omega_{i3}]^T \in \mathbb{R}^3$ stand for the spacecraft attitude described by MRPs and the angular velocity, respectively.

Remark 1. *MRPs is expressed as $\sigma_i = E_i \tan(\theta_i/4)$, where E_i is Euler axis of the attitude rotation and θ_i is Euler angular with satisfying $\theta_i \in (-2\pi, 2\pi)$. It should be noted that the attitude denoted by MRPs will be singular when θ_i is close to $\pm 2\pi$. As shown in [27], a corresponding vector $\sigma_i^s = -\sigma_i/\sigma_i^T\sigma_i$ of the original MRPs vector σ_i is introduced and the singularity problem is able to be solved by choosing to switch the MRPs when $\sigma_i^T\sigma_i > 1$.*

To facilitate the design of the SFF system, the following assumptions are introduced:

Assumption 2. *The generalized angular velocity is assumed to satisfy that $\|\omega\| \le \delta_1$, $\|\dot{\sigma}\| \le \delta_1$, where δ_1 is a positive constant.*

Assumption 3. *The generalized angular acceleration is assumed to satisfy that $\|\dot{\omega}\| < \delta_2$ and $\|\ddot{\sigma}\| < \delta_2$, in which $\delta_2 > 0$* is constant.

Assumption 4. *For the reference signal, the derivative of the reference angular acceleration is assumed to be bounded with satisfying $\|\ddot{\omega}_d\| \le \delta_3$, where $\delta_3 > 0$ is a constant.*

Remark 2. *Assumptions 2 and 4 are general which can be found in [7,28] respectively. Assumption 3 is reasonable because the control torque of each spacecraft has an upper bound, which means that the angular acceleration is bounded.*

Define the reference attitude and the reference angular velocity as σ_d and ω_d, respectively. For ith spacecraft, the tracking errors of attitude and angular velocity are defined as:

$$\sigma_{ei} = \sigma_i - \sigma_d \tag{4}$$

$$\omega_{ei} = \omega_i - \omega_d \tag{5}$$

Considering the SFF system subject to limited energy and computing resources, the control objective is to establish an event-based attitude coordination controller to realize attitude coordination and drive the system state errors σ_{ei} and ω_{ei} to arrive at a neighborhood around the origin.

3. Main Results

In this section, an attitude cooperative control algorithm with event-triggered strategy for SFF is proposed such that all spacecraft in formation achieve attitude synchronization. Before proceeding, the following two auxiliary variables are introduced, given by:

$$e_i = \sum_{j=1}^{n} a_{ij}(\sigma_i - \sigma_j) + \sigma_{ei} \tag{6}$$

$$\chi_i = \omega_{ei} + re_i \tag{7}$$

where $r > 0$ is constant and a_{ij} denotes the element of the weighted adjacency matrix A. $r > 0$ is to make σ_{ei} converge to a small bound of the origin after χ_i approaches zero.

Based on (3) and (5)–(7), we obtain:

$$\begin{aligned} J_i\dot{\chi}_i &= J_i(\dot{\omega}_i - \dot{\omega}_d) + rJ_i\dot{e}_i \\ &= u_i - {\omega_i}^{\times} J_i\omega_i - J_i\dot{\omega}_d + rJ_i\dot{e}_i \end{aligned} \tag{8}$$

For ith spacecraft, t_k^i represents the kth $(k = 1, 2, 3, \cdots)$ triggering time instant. The sampling values of e_i and χ_i are denoted by $\hat{e}_i$ and $\hat{\chi}_i$, which are defined, respectively, as:

$$\hat{e}_i = e_i\left(t_k^i\right) \tag{9}$$

$$\hat{\chi}_i = \omega_{ei}\left(t_k^i\right) + r\hat{e}_i \tag{10}$$

for all $t \in \left[t_k^i, t_{k+1}^i\right)$, where t_{k+1}^i denotes the next trigger moment.

A distributed event-based attitude coordinated controller is established for SFF with limited energy and computation resources, which is given by:

$$u_i(t) = -k_i\hat{\chi}_i - rJ_i\dot{\hat{e}}_i + \omega_i^{\times}\left(t_k^i\right)J_i\omega_i\left(t_k^i\right) + J_i\dot{\omega}_d\left(t_k^i\right) \tag{11}$$

where $k_i = k_0 + r\|J_i\| + 1$ and k_0 is a positive constant. Then, define the estimation errors of $\dot{e}_i$, χ_i, and ${\omega_i}^{\times}J_i\omega_i + J_i\dot{\omega}_d$ as $\dot{\widetilde{e}}_i$, $\widetilde{\chi}_i$, and $\widetilde{\eta}_i$, respectively. The estimation errors are given by:

$$\dot{\widetilde{e}}_i = \dot{\hat{e}}_i - \dot{e}_i \tag{12}$$

$$\widetilde{\chi}_i = \hat{\chi}_i - \chi_i \tag{13}$$

$$\widetilde{\eta}_i = \omega_i^{\times}\left(t_k^i\right)J_i\omega_i\left(t_k^i\right) + J_i\dot{\omega}_d\left(t_k^i\right) - {\omega_i}^{\times}J_i\omega_i - J_i\dot{\omega}_d \tag{14}$$

Subsequently, the event-triggered strategy of ith spacecraft is designed as:

$$t_{k+1}^i = \inf\left\{t > t_k^i \middle| \|\widetilde{\chi}_i\| + \left\|\dot{\widetilde{e}}_i\right\| + \|\widetilde{\eta}_i\| \geq \frac{\sqrt{2}}{2}\|\hat{\chi}_i\| + c_1e^{-c_2\tanh(t)}\right\} \tag{15}$$

where $c_1 > 0$ and $c_2 > 0$ are constants. c_1 and c_2 are designed as positive constants such that $c_1e^{-c_2\tanh(t)}$ keeps monotone positive decreasing, which will make the upper bounds of the system states errors smaller and smaller over time.

Remark 3. *Under the developed event-triggered strategy (15), the latest state information about its neighbors is only required in the calculation of the event-triggered function, which means that the calculation of the event-triggered strategy requires less energy and computing resources. In addition, the controller is only updated at its own triggering instants, which greatly reduces energy consumption and computational burden. When the event-triggered strategy (15) is satisfied, each spacecraft broadcasts the state information to its adjacent spacecraft and obtains state information about its adjacent spacecraft to make* $\|\widetilde{\chi}_i\| + \left\|\dot{\widetilde{e}}_i\right\| + \|\widetilde{\eta}_i\|$ *reset to zero.*

Theorem 1. *Consider the SFF system described by (1)–(3), the event-driven cooperative control scheme is constructed according to (11) and the event-triggered function is designed as (15). Then, the system trajectories are able to reach the neighborhood near the origin.*

Proof. Consider the following Lyapunov function:

$$V = \sum_{i=1}^{n}\chi_i^TJ_i\chi_i \tag{16}$$

In accordance with (8) and (11), taking the derivative of V gives:

$$\begin{aligned}\dot{V} &= 2\sum_{i=1}^{n}\chi_i^T J_i\dot{\chi}_i \\ &= 2\sum_{i=1}^{n}\chi_i^T\left(u_i - \omega_i{}^{\times}J_i\omega_i - J_i\dot{\omega}_d + rJ_i\dot{e}_i\right) \\ &= 2\sum_{i=1}^{n}\chi_i^T\left(-k_i\hat{\chi}_i - rJ_i\dot{\widetilde{e}}_i + \widetilde{\eta}_i\right)\end{aligned} \tag{17}$$

From the definition of χ_i, $\hat{\chi}_i$, and $\widetilde{\chi}_i$, we can get:

$$\begin{aligned}2\chi_i^T\hat{\chi}_i &= \chi_i^T(\chi_i + \widetilde{\chi}_i) + (\hat{\chi}_i - \widetilde{\chi}_i)^T\hat{\chi}_i \\ &= \chi_i^T\chi_i + \hat{\chi}_i^T\hat{\chi}_i + (\chi_i^T\widetilde{\chi}_i - \widetilde{\chi}_i^T\hat{\chi}_i) \\ &= \chi_i^T\chi_i + \hat{\chi}_i^T\hat{\chi}_i + (\widetilde{\chi}_i^T\chi_i - \widetilde{\chi}_i^T\hat{\chi}_i) \\ &= \chi_i^T\chi_i + \hat{\chi}_i^T\hat{\chi}_i - \widetilde{\chi}_i^T\widetilde{\chi}_i\end{aligned} \tag{18}$$

Substituting (18) into (17), we have:

$$\begin{aligned}\dot{V} &= -\sum_{i=1}^{n}k_i\chi_i^T\chi_i - \sum_{i=1}^{n}k_i\hat{\chi}_i^T\hat{\chi}_i + \sum_{i=1}^{n}k_i\widetilde{\chi}_i^T\widetilde{\chi}_i + 2\sum_{i=1}^{n}\chi_i^T\left(-rJ_i\dot{\widetilde{e}}_i + \widetilde{\eta}_i\right) \\ &\le -\sum_{i=1}^{n}k_i\|\chi_i\|^2 - \sum_{i=1}^{n}k_i\|\hat{\chi}_i\|^2 + \sum_{i=1}^{n}k_i\|\widetilde{\chi}_i\|^2 + 2\sum_{i=1}^{n}\|\chi_i\|\left(r\|J_i\|\left\|\dot{\widetilde{e}}_i\right\| + \|\widetilde{\eta}_i\|\right)\end{aligned} \tag{19}$$

Based on Young's inequality, we get:

$$\|\chi_i\|\left\|\dot{\widetilde{e}}_i\right\| \le \frac{1}{2}\left(\|\chi_i\|^2 + \left\|\dot{\widetilde{e}}_i\right\|^2\right) \tag{20}$$

$$\|\chi_i\|\|\widetilde{\eta}_i\| \le \frac{1}{2}\left(\|\chi_i\|^2 + \|\widetilde{\eta}_i\|^2\right) \tag{21}$$

Then, substituting (20) and (21) into (19) gives:

$$\begin{aligned}\dot{V} &\le -\sum_{i=1}^{n}k_i\|\chi_i\|^2 - \sum_{i=1}^{n}k_i\|\hat{\chi}_i\|^2 + \sum_{i=1}^{n}k_i\|\widetilde{\chi}_i\|^2 + \sum_{i=1}^{n}r\|J_i\|\left(\|\chi_i\|^2 + \left\|\dot{\widetilde{e}}_i\right\|^2\right) + \sum_{i=1}^{n}\left(\|\chi_i\|^2 + \|\widetilde{\eta}_i\|^2\right) \\ &= -\sum_{i=1}^{n}(k_i - r\|J_i\| - 1)\|\chi_i\|^2 - \sum_{i=1}^{n}k_i\|\hat{\chi}_i\|^2 + \sum_{i=1}^{n}k_i\|\widetilde{\chi}_i\|^2 + \sum_{i=1}^{n}r\|J_i\|\left\|\dot{\widetilde{e}}_i\right\|^2 + \sum_{i=1}^{n}\|\widetilde{\eta}_i\|^2\end{aligned} \tag{22}$$

Define $\alpha_{1i}^2 = k_i$ and $\alpha_{2i}^2 = r\|J_i\|$, where α_{1i} and α_{2i} are positive. According to the definition of k_i, it is obvious that $\alpha_{1i} > \alpha_{2i}$ and $\alpha_{1i} > 1$ hold true. Moreover, if $x > 0$, $y > 0$, and $z > 0$, the inequality $x^2 + y^2 + z^2 \le (x + y + z)^2$ holds. According to the above analysis, (22) can be recast as:

$$\begin{aligned}\dot{V} &\le -\sum_{i=1}^{n}k_0\|\chi_i\|^2 - \sum_{i=1}^{n}k_i\|\hat{\chi}_i\|^2 + \sum_{i=1}^{n}\left(\alpha_{1i}\|\widetilde{\chi}_i\| + \alpha_{2i}\left\|\dot{\widetilde{e}}_i\right\| + \|\widetilde{\eta}_i\|\right)^2 \\ &\le -\sum_{i=1}^{n}k_0\|\chi_i\|^2 - \sum_{i=1}^{n}k_i\|\hat{\chi}_i\|^2 + \sum_{i=1}^{n}k_i\left(\|\widetilde{\chi}_i\| + \left\|\dot{\widetilde{e}}_i\right\| + \|\widetilde{\eta}_i\|\right)^2\end{aligned} \tag{23}$$

From the proposed event-driven strategy (15), we obtain:

$$\|\widetilde{\chi}_i\| + \left\|\dot{\widetilde{e}}_i\right\| + \|\widetilde{\eta}_i\| \le \frac{\sqrt{2}}{2}\|\hat{\chi}_i\| + c_1e^{-c_2\tanh(t)} \tag{24}$$

Combining (23) and (24), we have:

$$\begin{aligned}\dot{V} &\leq -\sum_{i=1}^{n} k_0\|\chi_i\|^2 - \sum_{i=1}^{n} k_i\|\hat{\chi}_i\|^2 + \sum_{i=1}^{n} k_i\left(\frac{\sqrt{2}}{2}\|\hat{\chi}_i\| + c_1 e^{-c_2\tanh(t)}\right)^2 \\ &\leq -\sum_{i=1}^{n} k_0\|\chi_i\|^2 - \sum_{i=1}^{n} k_i\|\hat{\chi}_i\|^2 + 2\sum_{i=1}^{n} k_i\left[\left(\frac{\sqrt{2}}{2}\|\hat{\chi}_i\|\right)^2 + \left(c_1 e^{-c_2\tanh(t)}\right)^2\right] \\ &= -\sum_{i=1}^{n} k_0\|\chi_i\|^2 - \sum_{i=1}^{n} k_i\|\hat{\chi}_i\|^2 + \sum_{i=1}^{n} k_i\left[\|\hat{\chi}_i\|^2 + 2\left(c_1 e^{-c_2\tanh(t)}\right)^2\right] \\ &= -\sum_{i=1}^{n} k_0\|\chi_i\|^2 + 2\left(c_1 e^{-c_2\tanh(t)}\right)^2\sum_{i=1}^{n} k_i\end{aligned} \tag{25}$$

Define $k_{\max} = \max(k_1, k_2, \cdots, k_n)$ and $J_{\max} = \max(\|J_1\|, \|J_2\|, \cdots, \|J_n\|)$. The above equation can be rewritten as:

$$\begin{aligned}\dot{V} &\leq -\frac{k_0}{J_{\max}}\sum_{i=1}^{n} J_{\max}\|\chi_i\|^2 + 2n\left(c_1 e^{-c_2\tanh(t)}\right)^2 k_{\max} \\ &\leq -\mu V + \Delta\end{aligned} \tag{26}$$

where $\mu = k_0/J_{\max}$ and $\Delta = 2n\left(c_1 e^{-c_2\tanh(t)}\right)^2 k_{\max}$. Integrating (26) gives:

$$V(t) \leq \left(V(0) - \frac{\Delta}{\mu}\right)e^{-\mu t} + \frac{\Delta}{\mu} \tag{27}$$

From (27), we can conclude that the state errors of the SFF system are able to converge to the desired neighborhood under the proposed controller (11) with the developed event-triggered mechanism (15). The proof of Theorem 1 is completed.□

Remark 4. *It is important to realize that the design parameters c_1 and c_2 influence the inter-event time and the control performance simultaneously because the trigger threshold $c_1 e^{-c_2\tanh(t)}$ depends on c_1 and c_2 [29]. For one thing, the increase of c_1 and the decrease of c_2 are beneficial to the increase of the inter-event time, which means that the amount of computation will be reduced. For another, small c_1 and large c_2 will lead to good control performance, shrinking the convergence errors.*

For ith spacecraft, set the inter-event time among two consecutive events as $T_i = t_{k+1}^i - t_k^i$ and the minimum inter-event time (MIET) as $\tau_i^{\min}$, in which $\tau_i^{\min} \leq T_i$. In the following, the possibility of Zeno behavior can be excluded rigorously by proving that the MIET is positive.

Theorem 2. *For the SFF system (1)–(3) with the event-based attitude coordination control strategy (11) and the event-triggered mechanism (15), if Assumptions 1–4 hold true, the MIET $\tau_i^{\min}$ will be strictly positive, showing that the system has no Zeno phenomenon.*

Proof. Taking the derivative of $\|\widetilde{\chi}_i\|$ gives:

$$\frac{d\|\widetilde{\chi}_i\|}{dt} \leq \left\|\dot{\widetilde{\chi}}_i\right\| = \left\|\dot{\hat{\chi}}_i - \dot{\chi}_i\right\| = \|\dot{\chi}_i\| \tag{28}$$

According to (6) and (7), (28) can be rewritten as:

$$\begin{aligned}\frac{d\|\widetilde{\chi}_i\|}{dt} &\leq \left\|\dot{\omega}_{ei} + r\sum_{j=1}^{n} a_{ij}\left(\dot{\sigma}_i - \dot{\sigma}_j\right) + \dot{\sigma}_{ei}\right\| \\ &\leq \|\dot{\omega}_i\| + \|\dot{\omega}_d\| + nr\|\dot{\sigma}_i\| + nr\|\dot{\sigma}_j\| + \|\dot{\sigma}_i\| + \|\dot{\sigma}_d\| \\ &\leq 2(nr+1)\delta_1 + 2\delta_2\end{aligned} \tag{29}$$

Similarly, the derivative of $\left\|\dot{\widetilde{e}}_i\right\|$ is:

$$\begin{aligned}\frac{d\left\|\dot{\widetilde{e}}_i\right\|}{dt} \leq \left\|\ddot{\widetilde{e}}_i\right\| = \left\|\ddot{\hat{e}}_i - \ddot{e}_i\right\| = \|\ddot{e}_i\| &= \left\|\sum_{j=1}^{n} a_{ij}\left(\ddot{\sigma}_i - \ddot{\sigma}_j\right) + \ddot{\sigma}_{ei}\right\| \\ \leq n\left(\|\ddot{\sigma}_i\| + \|\ddot{\sigma}_j\|\right) + \|\ddot{\sigma}_i\| + \|\ddot{\sigma}_d\| &\leq 2(n+1)\delta_2\end{aligned} \tag{30}$$

The derivative of $\|\widetilde{\eta}_i\|$ is:

$$\begin{aligned}\frac{d\|\widetilde{\eta}_i\|}{dt} \leq \left\|\dot{\widetilde{\eta}}_i\right\| &= \left\|\frac{d\left(\omega_i^{\times}\left(t_k^i\right)J_i\omega_i\left(t_k^i\right) + J_i\dot{\omega}_d\left(t_k^i\right)\right)}{dt} - \frac{d\left(\omega_i{}^{\times}J_i\omega_i + J_i\dot{\omega}_d\right)}{dt}\right\| \\ &= \left\|\frac{d\left(\omega_i{}^{\times}J_i\omega_i + J_i\dot{\omega}_d\right)}{dt}\right\| \\ &= \left\|\dot{\omega}_i{}^{\times}J_i\omega_i + \omega_i{}^{\times}J_i\dot{\omega}_i + J_i\ddot{\omega}_d\right\| \\ &\leq \left\|\dot{\omega}_i{}^{\times}J_i\omega_i\right\| + \left\|\omega_i{}^{\times}J_i\dot{\omega}_i\right\| + \left\|J_i\ddot{\omega}_d\right\| \\ &\leq 2\|J_i\|\|\omega_i\|\left\|\dot{\omega}_i\right\| + \|J_i\|\left\|\ddot{\omega}_d\right\| \\ &\leq 2\|J_i\|\delta_1\delta_2 + \|J_i\|\delta_3\end{aligned} \tag{31}$$

In accordance with (29)–(31), we obtain:

$$\begin{aligned}\frac{d\|\widetilde{\chi}_i\|}{dt} + \frac{d\left\|\dot{\widetilde{e}}_i\right\|}{dt} + \frac{d\|\widetilde{\eta}_i\|}{dt} &\leq 2(nr+1)\delta_1 + 2\delta_2 + 2(n+1)\delta_2 + 2\|J_i\|\delta_1\delta_2 + \|J_i\|\delta_3 \\ &\leq 2(nr+1)\delta_1 + 2(n+2)\delta_2 + (2\delta_1\delta_2 + \delta_3)J_{\max}\end{aligned} \tag{32}$$

Define $\psi = 2(nr+1)\delta_1 + 2(n+2)\delta_2 + (2\delta_1\delta_2 + \delta_3)J_{\max}$. Integrating (32) with initial conditions $\widetilde{\chi}_i\left(t_k^i\right) = 0$, $\dot{\widetilde{e}}_i\left(t_k^i\right) = 0$, and $\widetilde{\eta}_i\left(t_k^i\right) = 0$ leads to:

$$\|\widetilde{\chi}_i\| + \left\|\dot{\widetilde{e}}_i\right\| + \|\widetilde{\eta}_i\| \leq \int_{t_k^i}^{t} \psi = \psi\left(t - t_k^i\right) \tag{33}$$

For all $t \in \left[t_k^i, t_{k+1}^i\right)$, $\|\widetilde{\chi}_i\| + \left\|\dot{\widetilde{e}}_i\right\| + \|\widetilde{\eta}_i\|$ grows from zero to $\frac{\sqrt{2}}{2}\|\hat{\chi}_i\| + c_1 e^{-c_2\tanh(t)}$. At the next triggering time $t = t_{k+1}^i$, (33) can be rearranged as:

$$\|\widetilde{\chi}_i\| + \left\|\dot{\widetilde{e}}_i\right\| + \|\widetilde{\eta}_i\| \leq \psi T_i \tag{34}$$

Based on the above analysis, we can get:

$$T_i \geq \frac{\sqrt{2}\|\hat{\chi}_i\|}{2\psi} + \frac{c_1 e^{-c_2\tanh(t)}}{\psi} \tag{35}$$

According to (35), we can set $\tau_i^{\min}$ as $\frac{c_1 e^{-\frac{c_2\pi}{2}}}{\psi}$, which is strictly positive, indicating that the SFF system is Zeno-free. This completes the proof of Theorem 2. □

4. Numerical Simulation

In this section, numerical simulations are come out to illustrate the superiority of the developed distributed event-triggered attitude coordinated controller. A SFF system including four spacecraft with the information flow presented in Figure 1 is considered.

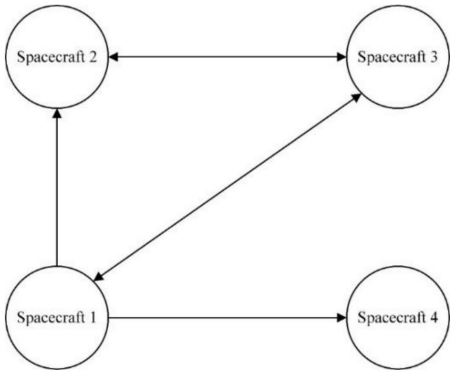

Figure 1. The communication topology.

From Figure 1, it is easy to obtain that matrices A and L are as follows:

$$A = \begin{bmatrix} 0 & 0 & 1 & 0 \\ 1 & 0 & 1 & 0 \\ 1 & 1 & 0 & 0 \\ 1 & 0 & 0 & 0 \end{bmatrix}, \; L = \begin{bmatrix} 1 & 0 & -1 & 0 \\ -1 & 2 & -1 & 0 \\ -1 & -1 & 2 & 0 \\ -1 & 0 & 0 & 1 \end{bmatrix}$$

The inertia matrices of formation spacecraft are described by:

$$\begin{aligned} J_1 &= diag(\begin{array}{ccc} 15 & 18 & 17 \end{array})\mathrm{kg}\cdot\mathrm{m}^2 \\ J_2 &= diag(\begin{array}{ccc} 16 & 19 & 14 \end{array})\mathrm{kg}\cdot\mathrm{m}^2 \\ J_3 &= diag(\begin{array}{ccc} 16 & 17 & 16 \end{array})\mathrm{kg}\cdot\mathrm{m}^2 \\ J_4 &= diag(\begin{array}{ccc} 17 & 19 & 15 \end{array})\mathrm{kg}\cdot\mathrm{m}^2 \end{aligned}$$

The initial attitude and initial angular velocity are given in Table 1. The reference attitude is set as $\sigma_d = [2\cos(0.1t) + 3, 3\sin(0.2t) + 1, -\sin(0.1t) + 2]^T \times 10^{-3}$ and the maximum output of the control input satisfies $|u_{ij}| \leq 2\mathrm{Nm}$, where $j = x, y, z$. The correlative design parameters are selected as: $r = 2$, $k_0 = 5$, $c_1 = 0.001$, and $c_2 = 1$ (Case 1). Figures 2 and 3 respectively illustrate that the attitude errors and angular velocity errors of four spacecraft are able to reach a neighborhood of the origin. The control signals of four spacecraft are presented in Figure 4. Finally, the triggering intervals of four spacecraft are illustrated in Figures 5–8.

Table 1. Initial attitude and initial angular velocity.

Spacecraft	Initial Attitude	Initial Angular Velocity
1	$\sigma_1(0) = [0.2, -0.15, 0.1]^T$	$\omega_1(0) = [0.03, 0.08, 0.1]^T \mathrm{rad/s}$
2	$\sigma_2(0) = [0.13, 0.16, 0.2]^T$	$\omega_2(0) = [0.02, -0.11, 0.07]^T \mathrm{rad/s}$
3	$\sigma_3(0) = [-0.15, 0.18, -0.16]^T$	$\omega_3(0) = [0.05, 0.06, -0.04]^T \mathrm{rad/s}$
4	$\sigma_4(0) = [-0.14, 0.12, 0.18]^T$	$\omega_4(0) = [-0.07, 0.09, 0.06]^T \mathrm{rad/s}$

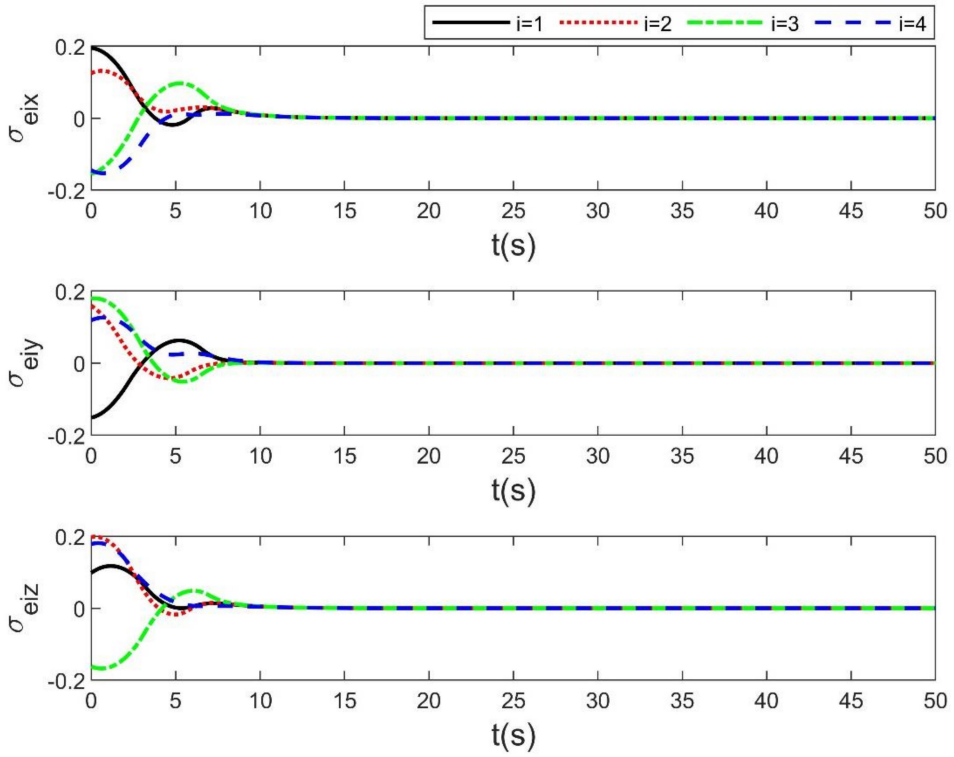

Figure 2. Case 1: The attitude errors of four spacecraft.

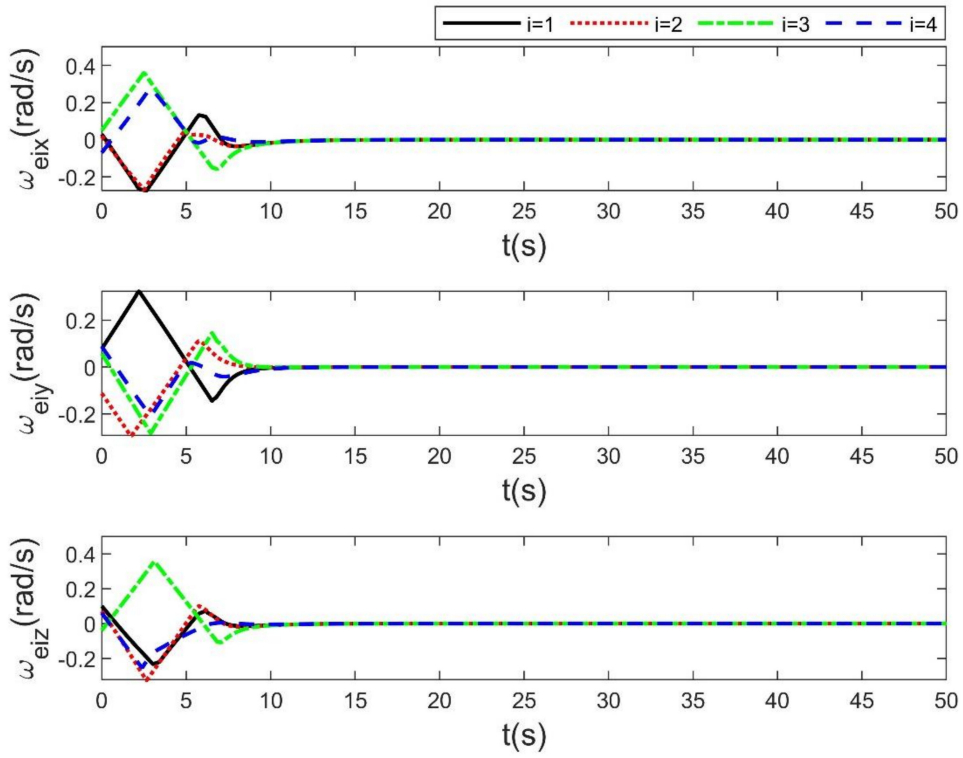

Figure 3. Case 1: The angular velocity errors of four spacecraft.

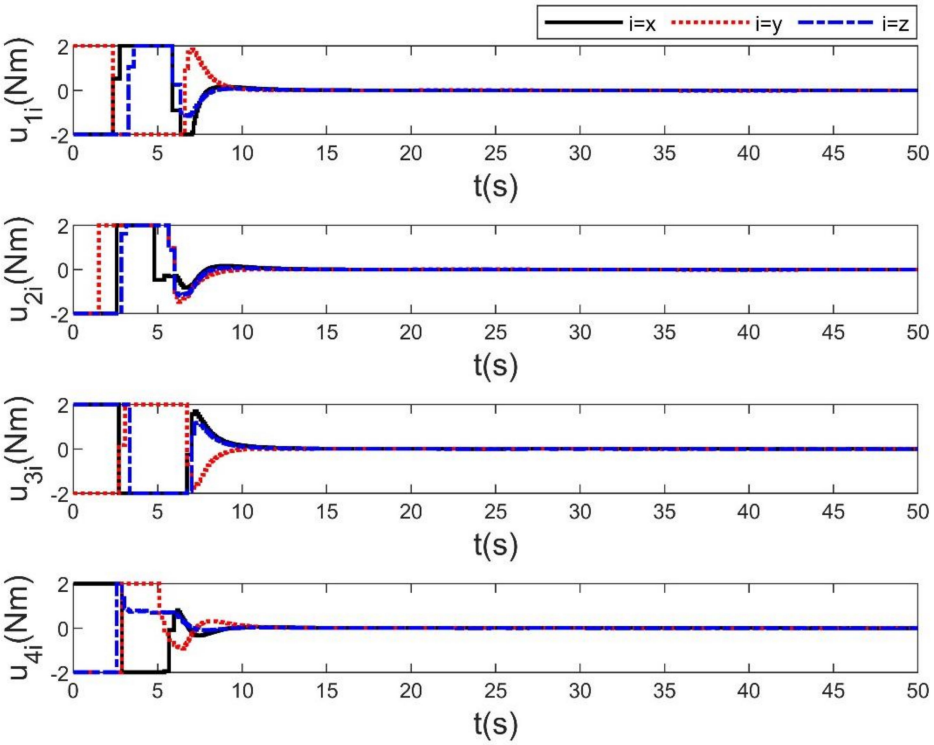

Figure 4. Case 1: Control signals of four spacecraft.

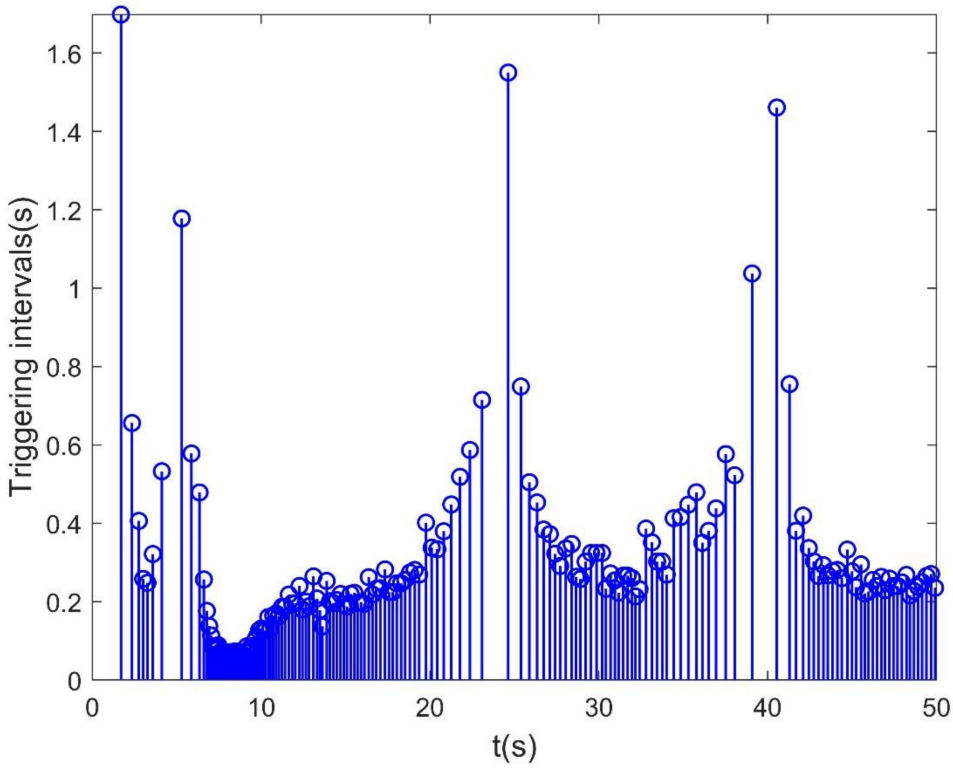

Figure 5. Case 1: Triggering intervals of spacecraft 1.

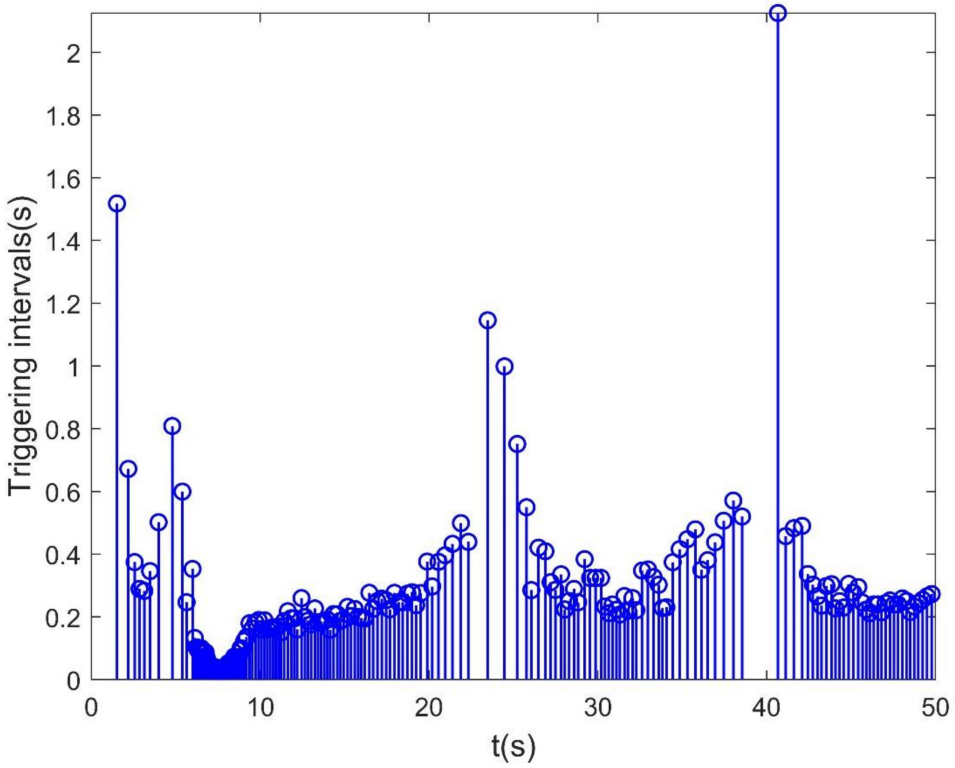

Figure 6. Case 1: Triggering intervals of spacecraft 2.

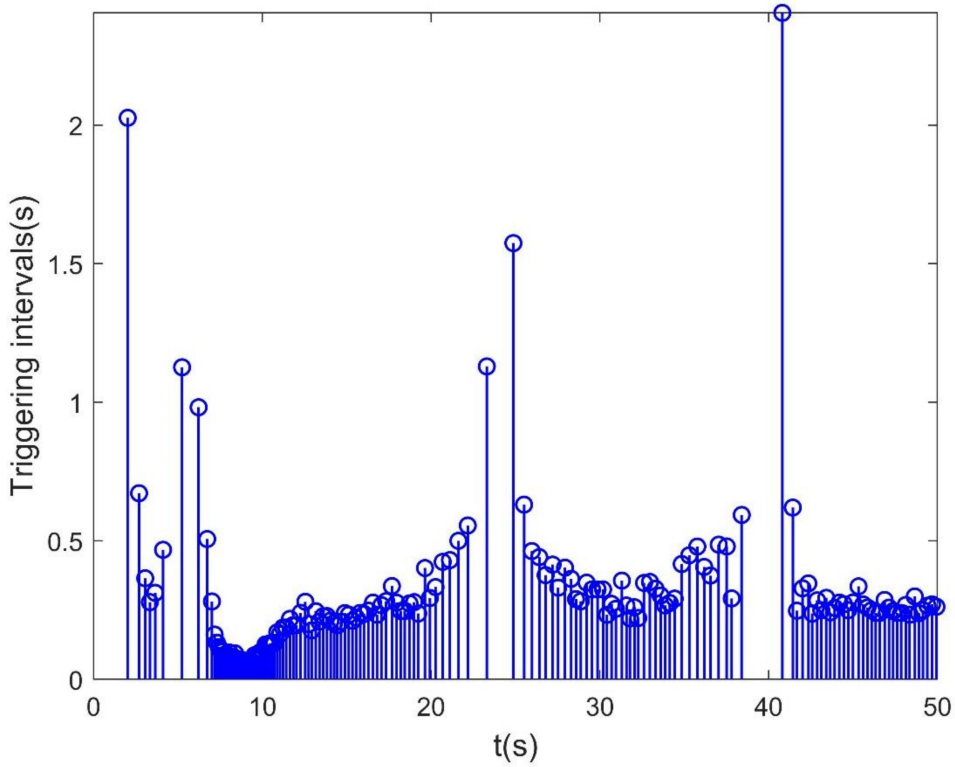

Figure 7. Case 1: Triggering intervals of spacecraft 3.

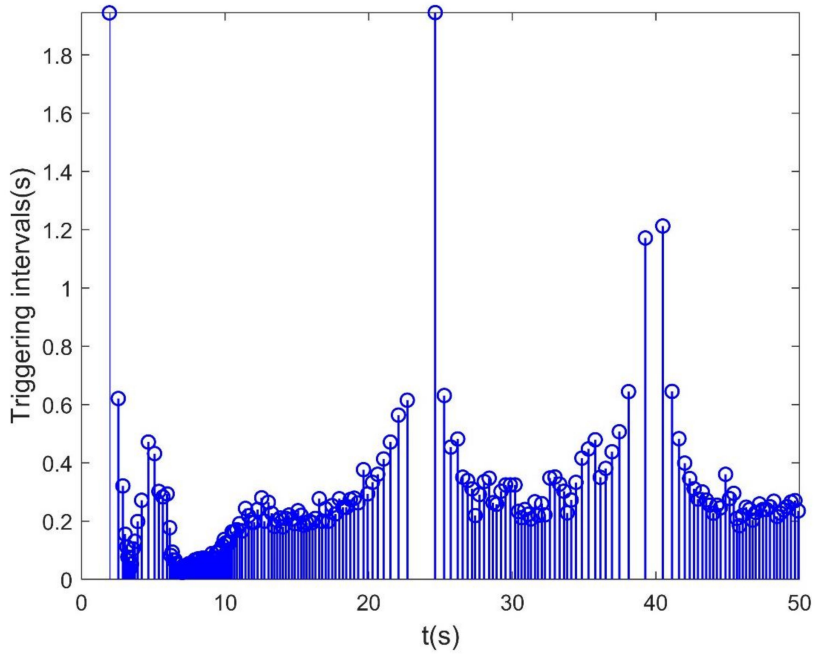

Figure 8. Case 1: Triggering intervals of spacecraft 4.

Recall that the design parameters c_1 and c_2 have an influence on the triggering interval and the convergence region. If the value of c_1 is larger and the value of c_2 is smaller, the triggering interval will be longer and the size of convergence region will be larger. Therefore, reset $c_1 = 0.01$, $c_2 = 0.1$, and other parameters remain unchanged (Case 2). The response curves of the attitude errors and angular velocity errors are displayed in Figures 9 and 10, respectively. The trajectories of control signals are plotted in Figure 11 and the triggering intervals are depicted in Figures 12–15.

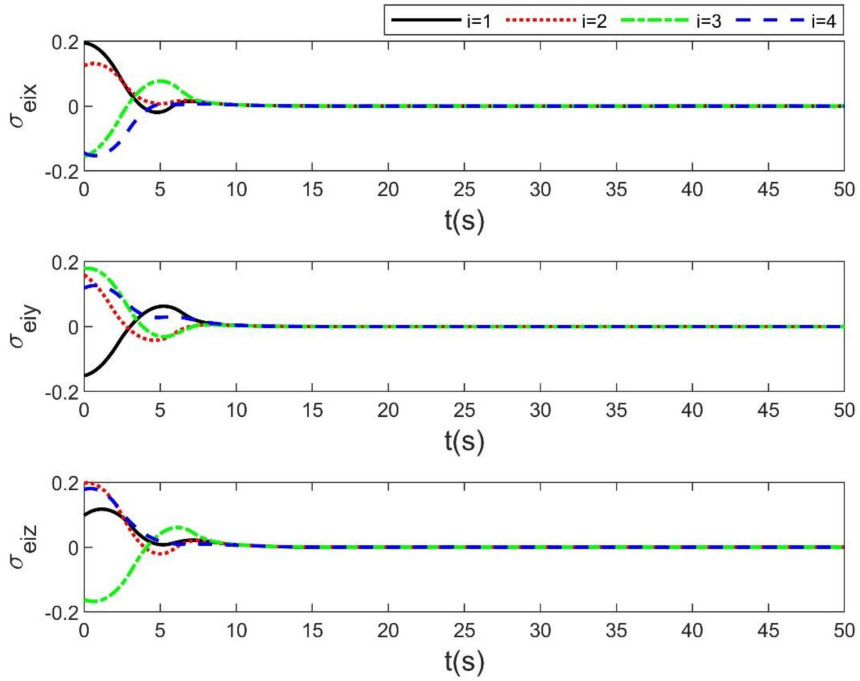

Figure 9. Case 2: The attitude errors of four spacecraft.

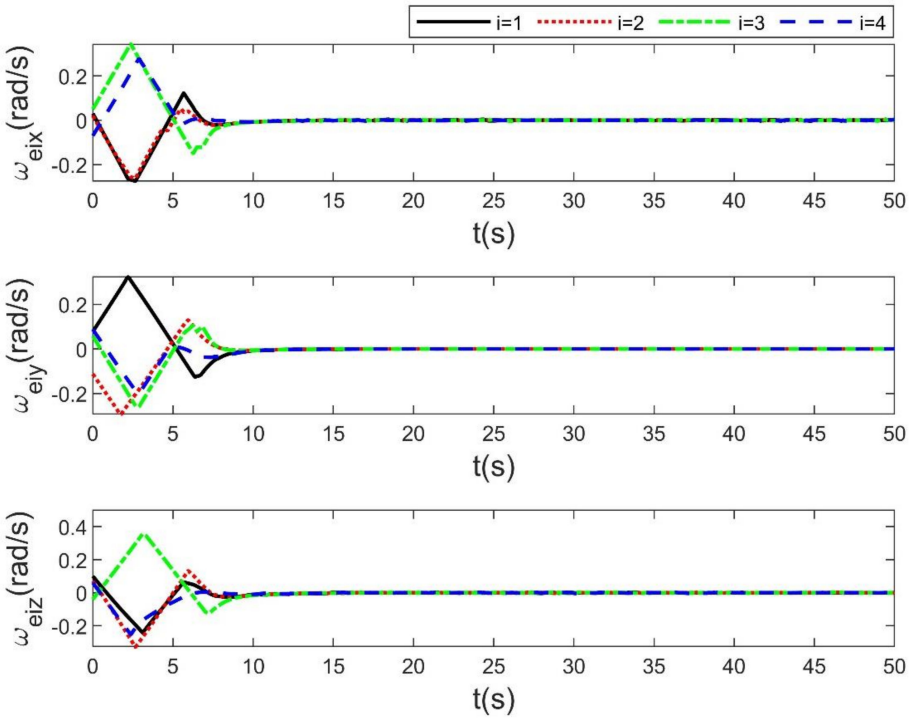

Figure 10. Case 2: The angular velocity errors of four spacecraft.

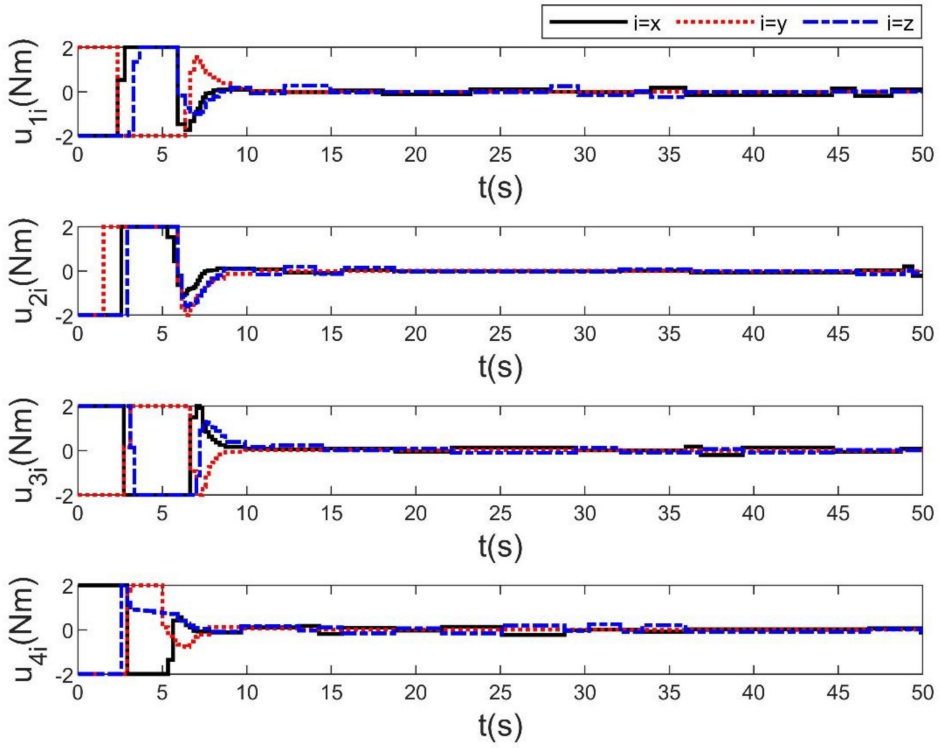

Figure 11. Case 2: Control signals of four spacecraft.

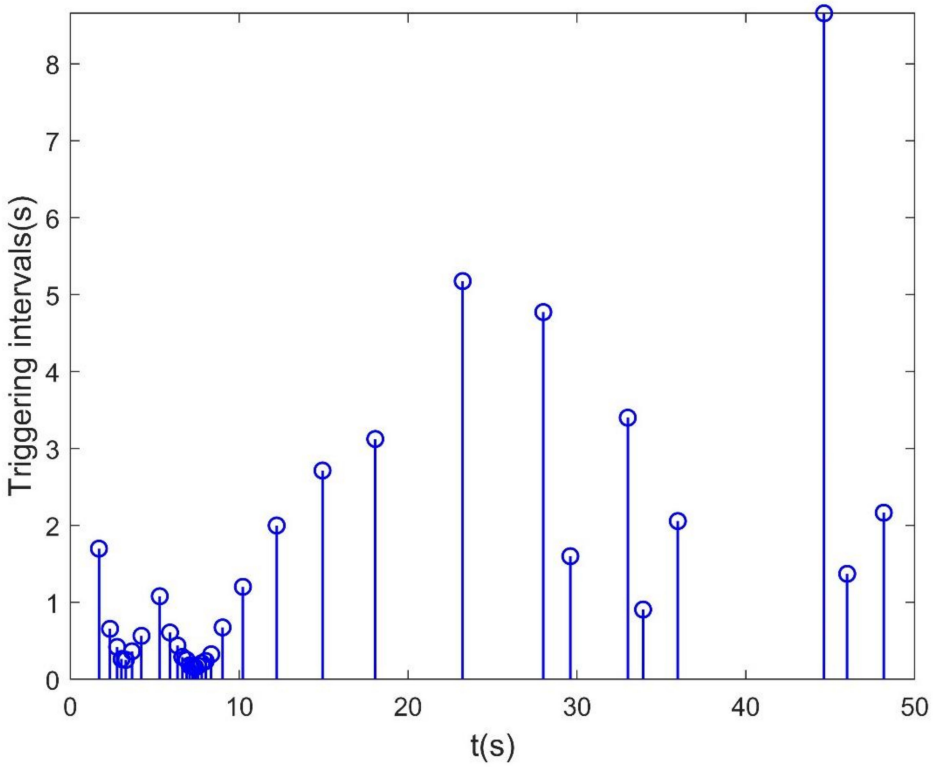

Figure 12. Case 2: Triggering intervals of spacecraft 1.

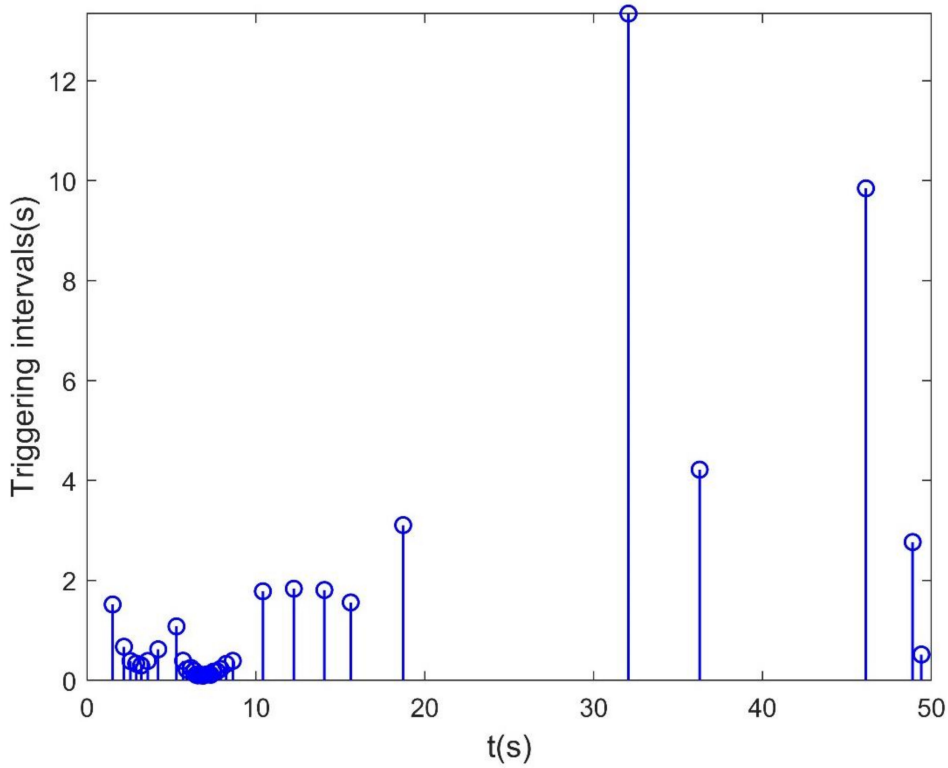

Figure 13. Case 2: Triggering intervals of spacecraft 2.

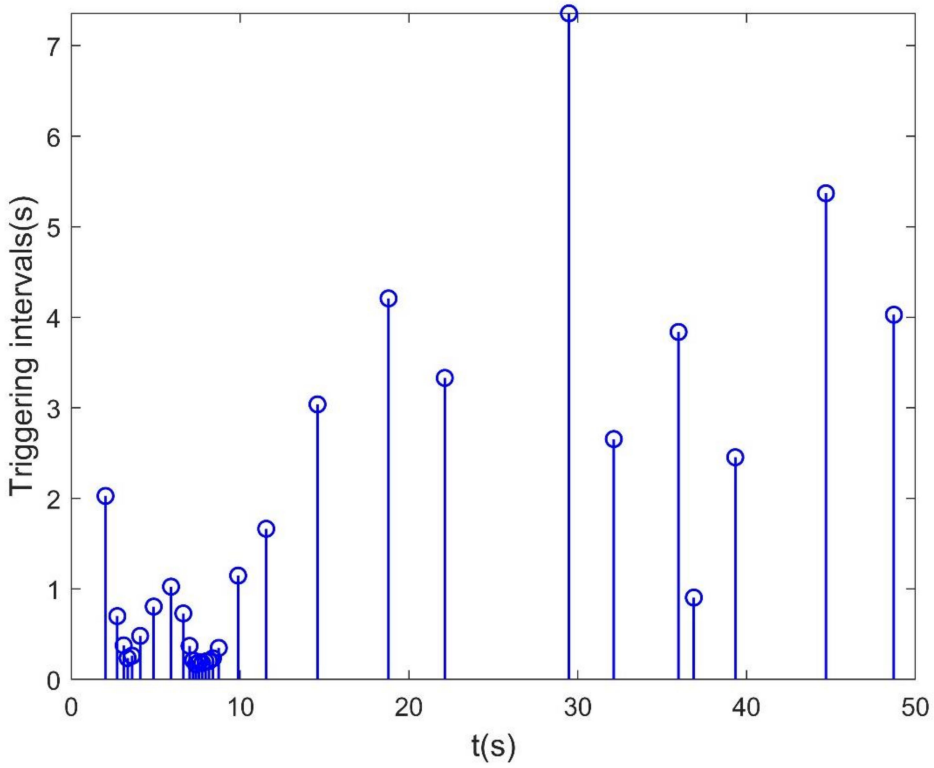

Figure 14. Case 2: Triggering intervals of spacecraft 3.

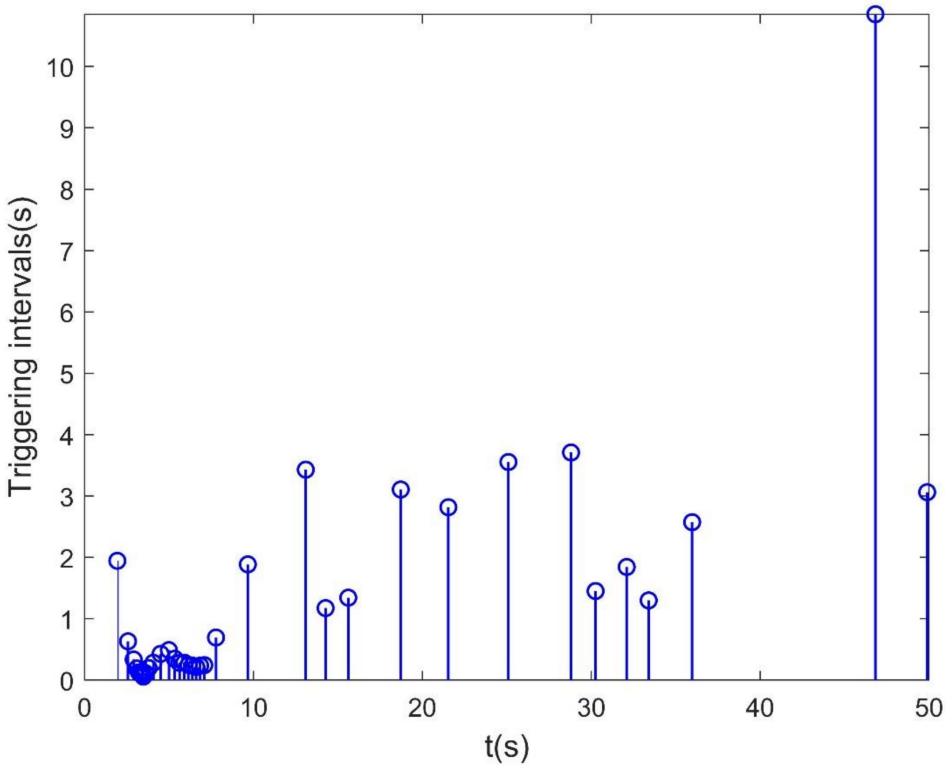

Figure 15. Case 2: Triggering intervals of spacecraft 4.

From Figures 2, 3, 9 and 10, one obtains that the system state errors are able to converge to the reference neighborhood around the origin and the attitude consensus can be achieved under the proposed controller. To present the advantages of the event-driven control scheme, the developed cooperative controller is executed in a time-driven manner

with a frequency of 10 Hz. In the simulation, the simulation time is chosen as 50 s, showing that the time-driven controller will be updated 500 times. Tables 2 and 3 show the detailed information about the inter-event time in two cases, respectively. From Tables 2 and 3, one can conclude that the inter-event time is increased as the parameter c_1 increases and the parameter c_2 decreases, and that the computation resources can be reduced by over 90% under the proposed event-driven controller by choosing appropriate design parameters. On the one hand, it should be emphasized that the ultimate convergence region is subject to parameters c_1 and c_2. Tables 4 and 5 respectively present the control performance of the proposed controller in two cases. Comparing Tables 4 and 5, one has that the control precision is reduced with the increase of c_1 and the decrease of c_2. Moreover, it should be emphasized that the average control inputs of Case 2 are much larger than the average control inputs of Case 1 after the control system is stable, which also shows that the control accuracy in Case 2 is higher than that in Case 1. Therefore, the values of c_1 and c_2 should be appropriate to achieve good control performance while saving computing and energy resources.

Table 2. Case 1: Triggering intervals of four spacecraft.

	Spacecraft 1	**Spacecraft 2**	**Spacecraft 3**	**Spacecraft 4**
Trigger number	181	203	170	217
Min interval (s)	0.052	0.027	0.057	0.024
Mean interval (s)	0.276	0.245	0.294	0.230
Max interval (s)	1.698	2.125	2.405	1.945
Reduction rate (%)	63.8	59.4	66.0	57.2

Table 3. Case 2: Triggering intervals of four spacecraft.

	Spacecraft 1	**Spacecraft 2**	**Spacecraft 3**	**Spacecraft 4**
Trigger number	33	36	30	36
Min interval (s)	0.154	0.094	0.167	0.057
Mean interval (s)	1.460	1.373	1.624	1.386
Max interval (s)	8.657	13.341	7.357	10.851
Reduction rate (%)	93.4	92.8	94.0	92.8

Table 4. Case 1: Control precision (15–50 s).

	$\|\|\sigma_{ei}\|\|_\infty$		$\|\|\omega_{ei}\|\|_\infty$**(Rad/s)**		$\|\|u_i\|\|_\infty$**(Nm)**	
	Mean	**Standard Deviation**	**Mean**	**Standard Deviation**	**Mean**	**Standard Deviation**
Spacecraft 1	4.1×10^{-5}	1.2×10^{-4}	9.5×10^{-5}	2.3×10^{-4}	6.4×10^{-3}	2.4×10^{-3}
Spacecraft 2	4.2×10^{-5}	1.2×10^{-4}	9.9×10^{-5}	2.3×10^{-4}	7.0×10^{-3}	2.8×10^{-3}
Spacecraft 3	4.1×10^{-5}	1.2×10^{-4}	9.6×10^{-5}	2.3×10^{-4}	6.5×10^{-3}	2.7×10^{-3}
Spacecraft 4	4.2×10^{-5}	1.1×10^{-4}	9.7×10^{-5}	2.2×10^{-4}	6.7×10^{-3}	2.6×10^{-3}

Table 5. Case 2: Control precision (15–50 s).

	$\|\|\sigma_{ei}\|\|_\infty$		$\|\|\omega_{ei}\|\|_\infty$**(Rad/s)**		$\|\|u_i\|\|_\infty$**(Nm)**	
	Mean	**Standard Deviation**	**Mean**	**Standard Deviation**	**Mean**	**Standard Deviation**
Spacecraft 1	2.2×10^{-4}	2.5×10^{-4}	1.4×10^{-3}	1.1×10^{-3}	0.15	0.058
Spacecraft 2	2.0×10^{-4}	2.8×10^{-4}	1.2×10^{-3}	9.0×10^{-4}	0.08	0.052
Spacecraft 3	2.0×10^{-4}	2.3×10^{-4}	1.2×10^{-3}	8.5×10^{-4}	0.12	0.046
Spacecraft 4	2.7×10^{-4}	2.7×10^{-4}	1.4×10^{-3}	9.9×10^{-4}	0.13	0.058

5. Conclusions

In this paper, an event-driven attitude coordinated control method has been established for multiple spacecraft systems subject to limited energy and computational resources under directed communication topologies. The uniformly ultimately bounded stabilization of the formation system has been guaranteed by Lyapunov theory and it has proved that the control system is able to achieve attitude synchronization under the proposed control strategy. In addition, an event-triggered strategy that does not require continuous state information of its neighbors has been designed to reduce the computational burden and the consumption of energy. Additionally, the inter-event time between two serial events has been proved to have a strictly positive lower bound, implying that the control system is Zeno-free under the developed event-based mechanism. Finally, numerical simulations are carried out to verify the proposed theoretical results. Compared with the time-driven method, the designed event-driven control scheme can make the closed-loop system save more than 90% computation resources and keep high-precision convergence of $\|\sigma_{ei}\|_\infty < 3 \times 10^{-4}$ and $\|\omega_{ei}\|_\infty < 2 \times 10^{-4}$ by selecting suitable design parameters. In the future, we will focus on the attitude consensus for multiple spacecraft systems subject to unknown disturbances and time-varying communication delays.

Author Contributions: X.X. and T.S. conceived of the presented idea; X.X. and L.H. designed the control algorithm and performed the simulation experiment. All authors wrote the manuscript. All authors have read and agreed to the published version of the manuscript.

Funding: This research was supported by the Major Program of National Natural Science Foundation of China (Grant Nos. 61690210, 61690213).

Institutional Review Board Statement: Not applicable.

Informed Consent Statement: Not applicable.

Data Availability Statement: The data used to support the findings of this study are available from the corresponding author upon request.

Conflicts of Interest: The authors declare no conflict of interest.

References

1. Hu, Q.L.; Shi, Y.X. Event-based coordinated control of spacecraft formation flying under limited communication. *Nonlinear Dyn.* **2020**, *99*, 2139–2159. [CrossRef]
2. Wang, J.; Zhang, R.N.; Yuan, J.P.; Luo, J.J. Multi-cubesat relative position and attitude determination based on array signal detection in formation flying. *IEEE Trans. Aerosp. Electron. Syst.* **2019**, *55*, 3378–3393. [CrossRef]
3. Liu, G.P.; Zhang, S.J. A survey on formation control of small satellites. *Proc. IEEE* **2018**, *106*, 440–457. [CrossRef]
4. Kim, S.W.; Park, S.Y.; Park, C. Spacecraft attitude control using neuro-fuzzy approximation of the optimal controllers. *Adv. Space Res.* **2016**, *57*, 137–152. [CrossRef]
5. Di Mauro, G.; Lawn, M.; Bevilacqua, R. Survey on guidance navigation and control requirements for spacecraft formation-flying missions. *J. Guid. Control Dyn.* **2018**, *41*, 581–602. [CrossRef]
6. Zhao, L.; Yu, J.P.; Shi, P. Command filtered backstepping-based attitude containment control for spacecraft formation. *IEEE Trans. Syst. Man Cybern. Syst.* **2021**, *51*, 1278–1287. [CrossRef]
7. Zou, A.M.; de Ruiter, A.H.J.; Kumar, K.D. Distributed finite-time velocity-free attitude coordination control for spacecraft formations. *Automatica* **2016**, *67*, 46–53. [CrossRef]
8. Lin, X.H.; Shi, X.P.; Li, S.L. Optimal cooperative control for formation flying spacecraft with collision avoidance. *Sci. Prog.* **2020**, *103*, 1–19. [CrossRef]
9. Chai, R.Q.; Tsourdos, A.; Savvaris, A.; Chai, S.C.; Xia, Y.Q.; Chen, C.L.P. Review of advanced guidance and control algorithms for space/aerospace vehicles. *Prog. Aerosp. Sci.* **2021**, *122*, 100696. [CrossRef]
10. Huang, N.; Duan, Z.S.; Zhao, Y. Distributed consensus for multiple Euler-Lagrange systems: An event-triggered approach. *Sci. China Technol. Sci.* **2016**, *59*, 33–44. [CrossRef]
11. Dimarogonas, D.V.; Tsiotras, P.; Kyriakopoulos, K.J. Leader-follower cooperative attitude control of multiple rigid bodies. *Syst. Control Lett.* **2009**, *58*, 429–435. [CrossRef]
12. Siavash, M.; Majd, V.J.; Tahmasebi, M. Fault-tolerant formation control of stochastic nonlinear multi-agent systems with time-varying weighted topology. *Trans. Inst. Meas. Control* **2020**, *42*, 1461–1474. [CrossRef]
13. Wang, W.J.; Li, C.J.; Sun, Y.C.; Ma, G.F. Distributed coordinated attitude tracking control for spacecraft formation with communication delays. *ISA Trans.* **2019**, *85*, 97–106. [CrossRef]

14. Zhang, C.X.; Wang, J.H.; Zhang, D.X.; Shao, X.W. Synchronization and tracking of multi-spacecraft formation attitude control using adaptive sliding mode. *Asian J. Control* **2019**, *21*, 832–846. [CrossRef]
15. He, X.Y.; Wang, Q.Y.; Hao, Y.Q. Finite-time adaptive formation control for multi-agent systems with uncertainties under collision avoidance and connectivity maintenance. *Sci. China Technol. Sci.* **2020**, *63*, 2305–2314. [CrossRef]
16. Lin, J.; Miao, Z.Q.; Zhong, H.; Peng, W.X.; Wang, Y.N.; Fierro, R. Adaptive image-based leader-follower formation control of mobile robots with visibility constraints. *IEEE Trans. Ind. Electron.* **2021**, *68*, 6010–6019. [CrossRef]
17. Nowzari, C.; Garcia, E.; Cortés, J. Event-triggered communication and control of networked systems for multi-agent consensus. *Automatica* **2019**, *105*, 1–27. [CrossRef]
18. Dimarogonas, D.V.; Frazzoli, E.; Johansson, K.H. Distributed event-triggered control for multi-agent systems. *IEEE Trans. Autom. Control* **2012**, *57*, 1291–1297. [CrossRef]
19. Wang, Y.W.; Lei, Y.; Bian, T.; Guan, Z.H. Distributed control of nonlinear multiagent systems with unknown and nonidentical control directions via event-triggered communication. *IEEE Trans. Cybern.* **2020**, *50*, 1820–1832. [CrossRef]
20. Zhang, C.X.; Wang, J.H.; Sun, R.; Zhang, D.X.; Shao, X.W. Multi-spacecraft attitude cooperative control using model-based event-triggered methodology. *Adv. Space Res.* **2018**, *62*, 2620–2630. [CrossRef]
21. Yang, R.H.; Zhang, H.; Feng, G.; Yan, H.C.; Wang, Z.P. Robust cooperative output regulation of multi-agent systems via adaptive event-triggered control. *Automatica* **2019**, *102*, 129–136. [CrossRef]
22. Nowzaria, C.; Cortés, J. Distributed event-triggered coordination for average consensus on weight-balanced digraphs. *Automatica* **2016**, *68*, 237–244. [CrossRef]
23. Wu, Z.G.; Xu, Y.; Lu, R.Q.; Wu, Y.Q.; Huang, T.W. Event-triggered control for consensus of multiagent systems with fixed/switching topologies. *IEEE Trans. Syst. Man Cybern. Syst.* **2018**, *48*, 1736–1746. [CrossRef]
24. Zhang, Y.H.; Li, H.Y.; Sun, J.; He, W. Cooperative adaptive event-triggered control for multiagent systems with actuator failures. *IEEE Trans. Syst. Man Cybern. Syst.* **2019**, *49*, 1759–1768. [CrossRef]
25. Yi, H.; Liu, M.; Li, M. Event-triggered fault tolerant control for spacecraft formation attitude synchronization with limited data communication. *Eur. J. Control* **2019**, *48*, 97–103. [CrossRef]
26. Zou, A.M.; Kumar, K.D. Distributed attitude coordination control for spacecraft formation flying. *IEEE Trans. Aerosp. Electron. Syst.* **2012**, *48*, 1329–1346. [CrossRef]
27. Schaub, H.; Akella, M.R.; Junkins, J.L. Adaptive control of nonlinear attitude motions realizing linear closed loop dynamics. *J. Guid. Control Dyn.* **2001**, *24*, 95–100. [CrossRef]
28. Li, B.; Qin, K.; Xiao, B.; Yang, Y.S. Finite-time Extended State Observer based fault tolerant output feedback control for attitude stabilization. *ISA Trans.* **2019**, *91*, 11–20. [CrossRef] [PubMed]
29. Liu, Y.; Jiang, B.X.; Lu, J.Q.; Cao, J.D.; Lu, G.P. Event-Triggered Sliding Mode Control for Attitude Stabilization of a Rigid Spacecraft. *IEEE Trans. Syst. Man Cybern. Syst.* **2020**, *50*, 3290–3299. [CrossRef]